

# Proposed Landslide Mapping Method for Canacona Region

P. M. Kessarkar, K. Srinivas, K. Suprit and  
A. K. Chaubey

National Institute of Oceanography,  
(Council of Scientific & Industrial Research),  
Dona Paula, Goa 403004.

18 February 2011



## Executive Summary

Following the catastrophic floods in Canacona taluka, the Government of Goa constituted the Canacona Flash Floods Study Committee to go into the causes of the event and to suggest remedial measures to enable better preparedness in the future. One of the recommendations made by the committee was to map areas vulnerable to mudslides and build site-specific disaster-management plans to face them for each such location. The committee recommended that this mapping study should be carried out using services of the faculty and students from Goan undergraduate and postgraduate institutions, and then circulated widely amongst local policy and decision makers.

One of the destructive geological processes, landslides, in general, include almost all varieties of mass movements on slopes, such as rock falls, rock slips, slumps, debris flows, etc. They have often been related to instability of slope, and sudden down-slope movement may be associated with highly water-saturated overburden containing debris material ranging in size from soil particles to gravel or boulders. Various researchers have listed a range of factors that are responsible for landslides; these factors are site-specific. These studies also indicate a trigger that finally initiates the movement.

In this report, an attempt has been made to (i) design a user-friendly method for the development of a landslide-susceptibility map, and (ii) understand the geological reasons behind the landslide that occurred in Canacona on 2 October 2009. The method is based on field observations in Kuskem, one of the landslide sites in the Canacona area. Six factors felt to be important for landslides, are short-listed. These factors are slope, height of terrain, vegetation, bedrock-overburden contact, soil type, and drainage pattern. To demarcate an area susceptible to landslides, the following steps are suggested. First, the area should be divided into small blocks or cells of appropriate resolution. Second, data sets should be generated for the above factors (the number of factors can be more in some cases) at the chosen resolution. Then, the factors should be ranked on a scale of 1 to 6 in order of importance, and weights should be assigned to classes of each factor. Third, based on the rank and weights, Landslide Potential Index (LPI) should be computed for each cell. Finally, LPI values should be classi-

fied into low, medium, high and very high landslide-susceptible classes using the LPI-frequency graph. In general, the proposed methodology will work for other regions as well. However, as noted above, landslide susceptibility is site-specific and regional factors have to be analyzed carefully before assigning ranks and weights to a specific region.

In this report, we have demonstrated the usefulness of the methodology using freely available existing datasets and tools on a grid resolution of  $90 \text{ m} \times 90 \text{ m}$ . The methodology is used to compute LPI to prepare a landslide susceptibility map for Canacona region. Although some of the input data were available only on a much coarser resolution, limiting the accuracy of LPI map, analysis shows that the major landslide events of 2 October 2009 occurred in regions with high values of LPI, validating the LPI map and the proposed method. The method can be extended to other regions on much finer resolutions by incorporating extensive data from field observations and remote-sensing.

# 1 Introduction

A landslide is a common natural hazard that results in loss of human lives and causes widespread damage to property and infrastructure. Landslides, in general, include all downward or sudden movement of surface material like clays, sand, gravel and rock. Earthquakes, heavy rainfall, volcanic eruptions, etc. may act as triggering mechanisms to initiate a landslide. The downward movement of surface material takes place under the influence of gravity, and the mobility of such movement is enhanced by water content in the sediment.

Canacona taluka in south Goa suffered from landslides and flash floods on 2 October 2009. A team consisting of geologists, surveyors, and students from the National Institute of Oceanography (NIO) visited the location of one landslide (Kuskem) to understand the reasons behind such an occurrence. The team also visited another landslide site near the locality. The NIO team collected information on various aspects and also visually made some observations. Based on the observations in the field, we suggest that the following geological aspects are pertinent for understanding the reasons behind the landslide.

Various researchers have studied landslides and concluded that several factors are important. An interested reader can refer to Thigale and Khandge (2005) and Kuriakose et al. (2009) for an overview of earlier studies that are relevant to the study of landslides. The factors identified in these studies were discerned based on field measurements and observations, but all the factors are not required to be measured everywhere when a landslide takes place. Some of the factors (like slope) are common and are useful for developing a methodology to understand the landslide.

In this report, we present a methodology (Sarkar and Kanungo, 2004) and procedure to compute Landslide Potential Index (LPI) and prepare a landslide-susceptibility map for the Canacona area. The basic principles, however, may be applied with modifications to other landslide-prone areas.

In order to prepare the landslide-susceptibility map, we used Geographic Information System (GIS), a powerful tool for visualisation and analysis of data. An open source and free GIS called GRASS GIS (Geographic Resources Analysis Support System) (Neteler and Mitasova, 2002) is used to calculate

the LPI. GRASS GIS is available for free download from the World Wide Web (<http://grass.fbk.eu/>).

First, we present specific observations made during the field trips by the NIO team. Subsequently, we describe the sources of data for each factor important for landslides in the Canacona taluka and provide a methodology to compute landslide susceptibility. Finally, we estimate the LPI and landslide susceptibility of Canacona region based on available data and suggested methodology.

## 2 Field work in Canacona area

Two hills from Kuskem in Canacona, where landslides occurred and damaged property, were selected for the ground-truth observations. The NIO team visited the first hill (Hill 1) on 6 April 2010 and the second (Hill 2) on 7 April 2010 (Figure 1).

### 2.1 Hill 1

The hill is located in Kuskem village (Figure 2). Before climbing the hill the team had a look at the river at the foot hills. The river bed is filled with large sized boulders and loose material. The boulders vary in size and are angular in shape.

The team followed the dried-up river bed towards the hill top. This facilitated visual observations of the bedrock and the nature of the overburden along the river banks. All along the journey up the hill, the team made several observations and measurements (shown as solid dots in Figure 1).

A brief summary of the observations made by the NIO team are as follows.

- (a) Near the foothill, the river bed was filled with rock boulders. The boulders consisted of crystalline rocks and lateritic boulders having a maximum size of  $1.5 \text{ m}^3$ . The exposed bed appeared to be schist. The strike and dip of the bed were measured with the help of a clinometer compass. The strike of the base rock was found to be  $\text{N}140^\circ$  with a dip angle of  $10^\circ$ , striking  $\text{N}60^\circ$ .

- (b) In the lower reaches, the bedrock of the hill was covered by thick overburden and the vegetation consisted of cashew trees. In the higher reaches, vegetation was either absent or scanty.
- (c) At the base of the hill, the nature and thickness of the overburden varied within a short distance. Lateritization of the bedrock (Schist) appeared to begin in the locations where the bedrock is exposed.
- (d) The team measured four sets of joints in the bedrock in the river bed. At places, the overburden consisted of loose soil that attained a maximum thickness of  $\sim 6$  m. The contact between the overburden and the bedrock was very sharp.
- (e) As the team proceeded further uphill, the river valley was found to be 10 m wide and 6 m deep. No loose rock or soil was observed other than the bedrock. At places, weathering structures like exfoliation were seen in the bedrock, which appeared to be granitic in nature and highly jointed. Lateritization was observed along these weak planes (joints).
- (f) Water was observed to be oozing at some locations and was percolating through the cracks of the bedrock.
- (g) Along the route, the team observed variation in the strikes and dips of the bedrock.
- (h) At the top of the hill where the landslide was initiated, the team observed minimum thickness of the sediment overburden and steep slopes ( $> 45^\circ$ ).

## 2.2 Hill 2

Hill 2 is located a couple of kilometres away from Kuskem village. On the way to this hill, the team observed a well that was excavated by the villagers for water. The section of the well was about 2.5 m and clearly depicted stratified layers of sediments and pebbles. Another site, about 100 m away from the previous one, exhibited debris slide over which vegetation had grown. Important observations on the hill are as follows:

- (a) Before reaching the hill, the team had to cross a river bed. The river bed was totally filled with boulders of a maximum size of  $\sim 1.5 \text{ m}^3$ ; there was loose sand on the banks and exposed green schists. Measured strike was  $\text{N}290^\circ$ .
- (b) For this hill, the team did not follow the river bed while climbing uphill. Since the river bed was not the route, the team did not find any exposed or cut sections en route to the hilltop. Thick vegetation covered the hill in general, except at those locations where a landslide had occurred.
- (c) Slope angles on the way appeared to change quite rapidly, and the maximum slope the team could measure was  $55^\circ$ .
- (d) The landslide on this hill had occurred from the top of the hill. At the starting point of the landslide, a part of the loose material was removed, forming a channel exposing the crystalline rocks at the base. The crystalline rock was highly laminated and dipped in one direction.

A regional assessment of the Canacona terrain and observations made on the hills 1 and 2 reveals the following factors which primarily govern slope instability in the region: slope of the terrain, height of the terrain, vegetation, bedrock-overburden contact, soil type, and drainage pattern.

## 3 Data

In this section, the factors considered in this study are discussed in detail. We have, however, combined the discussion of slope and height because they are estimated from the same data source. Similarly we have combined the discussion on bedrock-overburden contact and soil, as both are derived from an available soil map.

### 3.1 Slope and height of the terrain

Slope and height play an important role in governing the stability of a terrain. As the slope increases, chances of slope failure also increase. However, if two slopes have identical parameters except for elevation, the higher slope



with higher elevation will be more susceptible to a landslide. The degree of saturation of the slope-forming material is a major control over the occurrence of landslides. Slope face and slope angle were therefore considered important factors. On the west coast of India, west and north-west slope facets receive maximum rainfall, and are therefore more vulnerable to landslides. Steep slopes also expose fractured or fragmented rocks. The sources of information on elevation and slopes can be obtained from toposheets and field surveys. Relief of a surface can also be represented by a DEM (Digital Elevation Model), providing an alternate way to calculate the slope. DEMs are developed by remote-sensing techniques. A typical DEM represents the average height of the terrain in a grid cell. Although, DEMs are not as accurate as field surveys, they provide a broader picture of a region. Data from the field surveys and toposheets can be used to ascertain relative accuracy of the DEM.

### **3.1.1 Toposheets**

The toposheets are maps, typically of 1:25000 scale (depict smaller area with more details), and are published by the Survey of India. These maps provide information on drainage, roads, hills, forests, railway tracks, location of culverts, benchmarks (reference points), contours depicting elevation, etc. These maps are restricted in circulation. Contours shown on a toposheet can be digitized to prepare a digital contour database. The height of any feature depicted in toposheets is with reference to Mean Sea Level (MSL).

The slope of a line describes its steepness. A higher slope value indicates a steeper surface. On a toposheet, at the locations of higher slopes, the contours are closely packed and at the locations of lower slopes, the contours have wider separation.

### **3.1.2 Surveying**

An alternative to gathering information from toposheets is to carry out topographic surveying. Topographic surveying is a common practice for measuring heights, alignments, etc. The surveying is carried out using equipment like Total Station, Autolevels, LaserTrak<sup>TM</sup>, etc. (details in Appendix A).

Accuracy in measurements depends on the quality of the equipment deployed. The only limiting factor in topographic surveying is accessibility of the area.

### 3.1.3 Digital Elevation Model

A DEM is a digital representation of the earth's topography. It is derived using remote-sensing techniques such as radar data from satellites or airplanes (radar altimeter) and aerial photography. In India, the National Remote Sensing Centre (NRSC) at Hyderabad collects topographic data using satellites. These data can be used to prepare a digital representation of earth's topography. Another source of a high-resolution DEM is the National Aeronautics and Space Administration (NASA, USA), which provides free and easily accessible DEM data through the world wide web. One such DEM is the Shuttle Radar Topography Mission (SRTM) DEM, which is freely available for download from <http://www2.jpl.nasa.gov/srtm/>. An interested reader may visit the web sites (<http://srtm.csi.cgiar.org/> and <http://www2.jpl.nasa.gov/srtm/>) for more information (Farr et al., 2007). SRTM data is discussed in more detail in the other two sister reports.

We have used SRTM DEM for this study. It has a resolution of 3 arc second ( $90\text{ m} \times 90\text{ m}$  grid cells). The DEM was imported into the GRASS GIS and a topographic map of Goa was prepared (Figure 3). GRASS-GIS module “`r.slope.aspect`” was used to calculate the slope from the DEM for Goa. The module gives slope (inclination from horizontal) values in degrees for each of the grid cells. Slope is obtained by using an algorithm involving  $3 \times 3$  neighbourhood cells. A slope map for Canacona obtained by this method is presented in Figure 4. It is worth mentioning that slope values obtained by field measurements are more accurate than this method. The underestimation of slope estimated from a DEM is primarily due to averaging of height in a large grid cell ( $90 \times 90\text{ m}$ ) and the averaging algorithm ( $3 \times 3$  neighbourhood cells) used to calculate slope values. Nevertheless, in spite of the underestimation, the slope map (Figure 4) is able to resolve the geometry of the region quite well.

### 3.2 Vegetation (Land cover)

Dense vegetation cover prevents soil erosion by mechanical agents. It shields soil from the direct impact of rainfall and wind. Root systems increase the shear strength of the soil by binding through it. Vegetation also contributes to increased rainwater infiltration by increasing both the roughness of the surface and soil-mass permeability. Thus, densely vegetated areas are less susceptible to landslides than areas with barren soil cover. However, roots of some plants that penetrate down a potential slide plane, may also decrease the rock strength by facilitating weathering and loosening of soil.

Vegetation data for Goa was obtained from the Global Land Cover Facility's (GLCF, [www.landcover.org](http://www.landcover.org)) global land cover classification data. The global land cover classification data was generated by the University of Maryland's Department of Geography (UMD land cover classification). Satellite images acquired between 1981–1994 were analysed to distinguish fourteen land cover classes (Hansen et al., 1998, 2000) (Table 1). The data is available on a resolution of 1 km. To our knowledge, it is the highest resolution land cover data available presently free of cost. As a future plan, recent satellite images, which are available free, can be used (combined with ground truth data) to obtain higher resolution land cover data.

To conform to the SRTM DEM grid (resolution 90 m), the land cover map was re-sampled to the SRTM DEM grid (Figure 5) by nearest neighbourhood interpolation.

### 3.3 Bedrock-overburden contact and soil type

In stratigraphy, bedrock is the native consolidated rock underlying the surface. Overburden is the material that lies above the rock. The term overburden is also used to describe all soil and ancillary material above the bedrock horizon in a given area. In tropical regions, owing to monsoons, the bedrock or basement rock undergoes chemical weathering. The upper layers of the bedrock turn into reddish coloured rock, which is known as *laterite*. The nature and thickness of the lateritic profile solely depends on rain and the nature of the bedrock. The nature of the bedrock-overburden can be evaluated and observed at locations wherever it is exposed, for example, river

channels, road cuts, etc. The bedrock-overburden contact may be sharp, gradational or transitional in the increasing order of stability.

Canacona taluka is covered by rocks of Barcem formation of Dharwar Supergroup of Archean Proterozoic age (Gokul et al., 1985). The rock formations of this area consist of gneisses, metavolcanics, phyllites, schist, conglomerate, ferruginous quartzite and chert breccias. The rocks are folded into series of east-west trending synclines and anticline. These rocks are intruded by ultrabasic and basic sills and dykes, followed by Canacona granite and pegmatite (Srinivasan and Gopalkrishnan, 1985). These bedrock or the basement rocks are emplaced as batholiths, xenoliths, etc. Owing to weathering (mechanical or chemical), these rocks tend to develop weak zones in the form of joints, exfoliations, etc. The crystalline rocks develop weaker planes through which water can penetrate, weakening the joints further. Identification of these structures requires field study.

### **3.3.1 Soil: Nature of overburden**

Above the bedrock is usually an area of broken and weathered unconsolidated rock in the basal subsoil. Bedrock may weather below its upper surface, forming saprolites. The nature of the bedrock varies all along the Western Ghats. In Goa, most of the bedrock of the Western Ghats is overlain by red-coloured soil or rock of lateritic origin. The nature of lateritic profile and thickness varies according to the bedrock on which the overburden is formed.

The thickness of the overburden may vary from hard rock ( $\sim 30$ – $40$  m thick) intervened by phyllitic clays (as layers or as dykes) to very loose soil of small thickness ( $< 2$  m). The thickness of the overburden over a hill may be controlled by slopes of the hill. Over steep slopes, the overburden thickness is always less compared to thickness of the overburden in the region of gentle slopes. As mentioned earlier, the monsoon rains induce the chemical weathering of bedrock to form laterite. In a given area, the thickness of the overburden can be measured from exposed areas along the river channels, road cuts, etc. In case there are no exposures seen in the area of interest, it may be necessary to collect at least one core sample.

If the overburden is made up of loose material (not a hard lateritic rock),

it is recommended samples be collected at different places followed by sieve analysis. The sieve analyses are carried out to understand the texture of the overburden. The finest part of the samples (clay) is subjected to clay analyses to understand the nature of the clays. Some of the clays appear to swell when they come in contact with water and become more plastic in nature.

The hills of the Western Ghats in Goa, in general, comprise of laterites of various strengths, and lateritic soil as overburden above the basement rocks. Apart from laterite, clays also form an important part of this overburden. In the Canacona area, the overburden is observed to be loose soil in which the various types of rocks are embedded. On close observation, the loose soil is made up of coarse sand grains and occasional clays.

### **3.3.2 data**

An exhaustive field study is required to obtain the bedrock-overburden contact and soil data on a useful scale. Although remote sensing techniques can be used with ground truth observations to map the soils, for bedrock-overburden contact detailed observations are a must.

In this study, an available soil map of Goa (Harindranath et al., 1999) was used to obtain soil type for the region. This map is available in two sheets at a scale of 1:500,000 for the whole of Goa, where 25 different soil units are identified (Table 2). This map was digitised using GRASS GIS, and then converted into a raster map (Figure 6) of resolution  $90\text{ m} \times 90\text{ m}$  (same as SRTM DEM).

Bedrock-overburden contact data was primarily derived from our field survey in Kuskem. Information obtained from this field survey was correlated subjectively with detailed soil characteristics given in the soil map (Harindranath et al., 1999) and the bedrock-overburden contact was inferred.

The soil map used to obtain soil and bedrock-overburden contact data is a coarse resolution map. Such a small scale map gives average soil type or predominant soil type over a large area based on limited field observation. Data accuracy for these two factors, specially for bedrock-overburden contact, can be improved by conducting extensive field surveys. This will be very

useful in analysis on much finer resolutions.

### **3.4 Drainage pattern**

In geomorphology, a *drainage system* is the pattern formed by the streams, rivers, and lakes in a particular drainage basin. The pattern is governed by the topography and gradient of the terrain, and presence of hard or soft rocks. The drainage pattern is a common phenomenon in the areas of rough terrain that might have formed due to soil erosion over soft rock. The gullies associated with the drainage pattern facilitate the through flow of water and may be connected to a larger channel so as to form a dendritic type of drainage pattern. On the higher reaches of the hill, these gullies or channels appear to be subtle in nature, and the gullies become more pronounced as they reach the lower slopes. The number, shape, length and size of gullies and the main channel associated within a drainage basin of an area vary and can be traced on a topographic map. The presence or absence of a drainage pattern near the site of a landslide defines how fast and how far the landslide material can reach down the slopes, as these gullies or channel associated with the drainage pattern facilitate faster movement of landslide debris down the hill slopes.

Drainage pattern is derived from the stream network data. SRTM DEM is used to obtain the stream network using a hydrological modelling module `r.watershed` (detailed description of this module is given in the second sister report). Each stream grid cell is given a value of one and a non-stream grid cell a value of zero. To obtain the drainage density at a grid cell, total number of stream cells is calculated over a  $5 \times 5$  moving window neighbourhood. The resultant map (Figure 7) is an indicator of drainage density (true density can be obtained by dividing this value by the area of 25 grid cells).

## **4 Methodology for landslide susceptibility mapping**

A landslide-susceptibility map indicates relatively potential zones such as low, medium, high and very high for landslide occurrence. There could be

several approaches to prepare a landslide-susceptibility map. In the present study, the approach followed by Sarkar and Kanungo (2004) is used, considering primarily the local geology and geomorphology of Canacona area. Several parameters and their classes are chosen and weights are assigned according to their potential to cause a landslide (Table 3). Based on the data discussed in Section 3, GRASS GIS is used to calculate the Landslide Potential Index (LPI) for the Canacona region.

#### 4.1 Landslide Potential Index (LPI)

The landslide susceptibility map can be prepared by computing Landslide Potential Index (LPI) and classifying LPI into several landslide susceptible zones such as low, medium, high and very high. The LPI is defined as:

$$\text{LPI} = \sum_{i=1}^n (R_i W_i), \quad (4.1)$$

where  $R_i$  denotes the rank for factor  $i$  and  $W_i$  denotes the weight of class of factor  $i$ . In this study the total number of factors ( $n$ ) is 6, where weight of class varies from 0 to 6 (Table 3).

#### 4.2 Weights of factors for landslide

Ranks and weights of causative factors (parameters) need to be assigned in order to generate a landslide-susceptibility map. The important factors responsible for the Canacona landslides were assigned numerical values (rank) on a 1 to 6 scale in order of importance. Weights were assigned to the classes of the factors on 0 to 6 ordinal scales, where higher weight indicates a greater susceptibility to landslide occurrence. The details of ranks and weights for factors and their classes are presented in Table 3. After collecting pertinent data from the available sources described earlier, initial data maps (Figure 3 to Figure 7) were re-classed according to the weights given in Table 3. Re-classification of the slope map (Figure 8) and the elevation map (Figure 9) was straightforward as classification was based on the numerical values. For deriving the vegetation map (Figure 10), land cover classes (Table 1) 1 to 6 were assigned weight 1 (dense vegetation), 7 to 11 were assigned weight 3

(sparse vegetation), 12 to 13 were assigned weight 6 (barren) and water (sea or river) was assigned null weight.

Bedrock-overburden contact map (Figure 11) was derived using the soil map (Figure 6). For deriving bedrock-overburden contact, important soil units relevant to the Canacona region were 10 and 11 (weight assigned 1), 20 and 22 (weight assigned 3), 18 and 21 (weight assigned 6). Rest of the soil units were assigned weights either 1 (for soil of plain areas; soil units 1–17) or 6 (soils of hill areas; soil units 19 and 23–26) (Table 2). Re-classed map of soil was derived from the soil map (Figure 6 and Table 2). Soil units 7,8,10, and 22 were assigned weight 3; 1–4, 11–17, and 20 were assigned weight 4, and the rest of the soil units were assigned weight 6. The soil map (Harindranath et al., 1999) does not include the hard laterite soil class (weight 0), as observed in our field study of Kuskem, so there are no areas with weight 0 in this region.

Drainage pattern map (Figure 7) was re-classed into drainage density map (Figure 13) by assigning weights for region of high density (weight 6 for drainage greater than 100), medium (weight 3 for density between 50 and 100) and low density (weight 1 for density less than 50) (Figure 13). The thresholds were chosen subjectively based on the mean value ( $\sim 48$ ) and standard deviation ( $\sim 19$ ) of the density.

### 4.3 Computation of LPI map

The LPI is computed using the following steps.

- (a) The entire region is divided into grid cells. The cell size should represent the amount of detail one would like to see. A smaller cell size implies more exhaustive data requirement, and therefore, more analysis. In practice, the size of the grid cells depends upon the data availability. Since slope and elevation are two most important parameters for this region (Table 3), we have used the grid size ( $90 \times 90$  m) for all parameters due to availability of SRTM DEM in  $90 \times 90$  m grid size.
- (b) Assign rank and weights for the each factor. Maps of available factors are then re-classified in different categories and assigned weights according to Table 3.



- (c) Calculate LPI value for each cell to generate LPI map for the region. As an example, computation of maximum and minimum LPI based on the data shown in Table 3 is presented in Table 4.
- (d) The LPI values are classified into landslide-susceptible classes such as low, medium, high and very high using the LPI-frequency graph. The threshold values can be drawn at significant changes in the gradients of the graph and field observations on landslide occurrences.

Depending upon the data availability, quality of the landslide-susceptibility map may be improved by incorporating more factors, or assigning more classes of weight, if need arises. Furthermore, the landslide-susceptibility map should be updated periodically, because any changes in the natural environment by human interference may influence the changes in landslide susceptibility of the area.

The Landslide Potential Index (LPI) map derived for the Canacona region is shown in Figure 14. The LPI value ranges from 27 to 99 with an average value of 58 and standard deviation of 15. Locations where major landslides occurred on 2 October 2009 coincided with high values of LPI (Figure 14), thus validating the LPI maps. To identify the LPI-based landslide-susceptible classes, LPI-frequency graph is plotted (Figure 15). Based on the changes in the gradient of the LPI-frequency graph, four different classes of LPI thresholds were subjectively identified for landslide susceptibility. Grid cells with an LPI value of greater than or equal to 85 are identified as *very high* landslide susceptible areas. Grid cells with LPI value between 85 and 65 are identified as *high* landslide susceptible areas. Grid cells with LPI values between 65 and 40 are *medium* landslide susceptible areas. Grid cells with LPI value less than 40 have lowest landslide susceptibility. If sufficient field data on previous occurrence of landslides is available, more sophisticated statistical techniques can be used to derive the different susceptibility thresholds and the classification can be made more objective.

#### 4.4 Triggering mechanisms

Identifying the landslide-susceptible areas is an important aspect for preparedness for landslide events. However, merely identifying the landslide

susceptible areas will not be so useful for preventing loss of life and property, unless some sort of an early warning system is present. It may be mentioned here that, landslides are triggered by flash floods, earthquakes, volcanoes, etc. Thus, to provide an early warning, the role of triggering factors should also be considered.

Goa receives most of its rainfall (almost 90% of annual rainfall) during the summer monsoon (June–September). The distribution of rain is not even during the season: there are heavy showers on some days (at times, rainfall can exceed  $30 \text{ cm day}^{-1}$ ) and light showers on other days. It may be noted, however, that the rainfall is usually measured on the plains, but measurements are rare on hill slopes and ridges. The hills, being highly elevated features, receive more rainfall than the coastal plains (Suprit and Shankar, 2008). This increase in rainfall with elevation is seen elsewhere too. For example, the mean annual rainfall in the coastal plains of Hong Kong (China) is about 130 cm, whereas in the mountains it is about 300 cm (Chau et al., 2004), and landslides usually occur during or immediately after the heavy rainfall (Jamaludin et al., 2006). These heavy rains induce mechanical and/or chemical weathering of exposed bedrocks. The flows consist of movement of slurry soil and loose rocks down the slope in a manner analogous to a viscous fluid. Falls, on the other hand, are incidences of masses of rocks detaching from a steep slope and descending by free fall, rolling and bouncing (Jamaludin et al., 2006). Our study reveals that on 2 October 2009, unprecedented intense rainfall (271 mm in 7 hours) was the triggering factor, which caused many landslides in the high landslide-susceptible regions of Canacona.

As mentioned earlier another important possible landslide triggering mechanism is an earthquake. Earthquake-related landslides are common in mountainous and hilly regions on the land and even under the sea. As everyone knows, the ground shakes during an earthquake and that causes lots of damage to property and also causes landslides under favourable conditions. In Goa, the India Meteorological Department (IMD) records and provides information on occurrence or absence of earthquakes at any given time. Our enquiry with IMD revealed that no earthquake occurred on 2 October 2009 in Goa. We therefore rule out earthquake as a triggering factor for this

landslide.

## 5 Conclusions

A methodology to compute the LPI and prepare a landslide-susceptibility map is presented. As per the map, Kuskem and Canacona have high susceptibility for landslide. The field survey and the fact that a landslide occurred confirm the usefulness of the LPI map. Steep slopes, high elevations and the sharp contact of the overburden with the base rock were the major factors that made this region susceptible to landslides. The intense rainfall event of 2 October 2009 served as a trigger for the landslides in Canacona.

The landslide susceptibility and LPI map, along with a watch-keeping mechanism for the rainfall (discussed in the third sister report), can be used to provide a useful warning for rainfall triggered landslides.

The methodology can be easily extended to estimate LPI over the rest of Goa. It uses free and readily available tools and data. Though the method can be applied quickly to generate LPI maps using readily available data (remotely-sensed, available maps, etc.), it suffers from the drawback that it is not very accurate owing to the coarser resolution datasets used. This is important if we want to make decisions on a large scale, like, deciding on the difference in LPI for locations 200 meters apart. To do this would require using much more accurate data for all the factors on finer scales and would demand extensive field surveys. So, it is important that the LPI estimated from available data are confirmed by field work as described in the report. We hope that the students and faculty from Goan undergraduate and postgraduate institutions will undertake such field work to verify LPI maps drawn with the technique described here and subsequently extend the methodology.

## 6 Acknowledgements

We thank Dr. S. R. Shetye, Director, NIO and Dr. D. Shankar, the Principal Investigator of this project, for support and encouragement. Our colleagues,

Mr. N. Prabhakaran, Mr. K. C. Pathak, Mr. Gavin Walker, Mr. Sripad Gaonkar, and students — Mr. Kiran Kumar Kanala, Mr. Alok Athavale and Mr. Aravind Kalla — provided support in the field observations. Mr. Aravind Kalla digitised the soil map of Goa. Thanks are due to Mr. V. Mahalingam for converting this document from OpenOffice to L<sup>A</sup>T<sub>E</sub>X. We acknowledge the role of GRASS GIS and other open source softwares used in this study. This work was funded by the Government of Goa.

## References

- K. T. Chau, Y. L. Sze, M. K. Fung, W.Y. Wong, E. L. Fong, and L. C. P. Chan. Landslide hazard analysis for Hong Kong using landslide inventory and GIS. *Computers and Geosciences*, 30:429–443, 2004. 18
- T. G. Farr, P. A. Rosen, E. Caro, R. Crippen, R. Duren, S. Hensley, M. Kobrick, M. Paller, E. Rodriguez, L. Roth, D. Seal, S. Shaffer, J. Shimada, and J. Umland. The Shuttle Radar Topography Mission. *Reviews of Geophysics*, 45(RG2004), 2007. doi: 10.1029/2005RG000183. 10
- A. R. Gokul, M. D. Srinivasan, K. Gopalkrishnan, and L. S. Vishwanathan. Stratigraphy and structure of Goa. In *Earth resources for Goa's development*, page 113, Hyderabad, 1985. 12
- M. R. Hansen, R. DeFries, J.R.G. Townshend, and R. Sohlberg. Umd global land cover classification. Technical report, Department of Geography, University of Maryland, College Park, Maryland, 1998. URL <http://glcf.umiacs.umd.edu/data/landcover/>. Product: 1 kilometer, Version: 1.0, Product coverage date: 1981–1994. 11, 24
- M. R. Hansen, R. DeFries, J.R.G. Townshend, and R. Sohlberg. Global land cover classification at 1km resolution using a decision tree classifier. *International Journal of Remote Sensing*, 21:1331–1365, 2000. 11, 24
- C. S. Harindranath, K. R. Venugopal, N. G. Raghumohan, J. Sehgal, and M. Velayutham. Soils of Goa for optimising land use. Technical report,

- National Bureau of Soil Survey and Land use planning, Nagpur, India, 1999. 2 Sheets of soil map on 1:500,000 scale. 13, 16, 25, 39
- S. Jamaludin, B. B. K. Huat, and H. Omar. Evaluation of slope assessment systems for predicting landslides of cut slopes in granitic and meta-sediment formations. *American Journal of Environmental Sciences*, 2: 135–141, 2006. 18
- S. L. Kuriakose, G. Sarkar, and C. Muraleedharan. History of landslide susceptibility and a chronology of landslide prone areas in the Western Ghats of Kerala, India. *Environmental Geology*, 57:1553–1568, 2009. doi: 10.1007/s00254-008-1431-9. 5
- M. Neteler and H. Mitasova. *Open Source GIS: A GRASS GIS Approach*. Kluwer Academic Publishers, Dordrecht, Netherlands, 2002. 5
- S. Sarkar and D. P. Kanungo. An integrated approach for landslide susceptibility mapping using remote sensing and GIS. *Journal of Photogrammetric Engineering & Remote Sensing*, 70(5):617–625, 2004. 5, 15
- M. D. Srinivasan and K. A. Gopalkrishnan. Geology of Canacona area with special reference to Canacona granite. In *Earth resources for Goa's development*, page 602, Hyderabad, 1985. 12
- K. Suprit and D. Shankar. Resolving orographic rainfall on the Indian west coast. *International Journal of Climatology*, 28:643–657, 2008. 18
- S. S. Thigale and A. S. Khandge. *Coping with natural hazards: Indian context*, chapter Coping with landslide disasters in the Western Ghats. Orient Longman, New Delhi, 2005. 5

## Appendix A Surveying techniques

Measurement of topography can be made with reference to a benchmark. Sometimes a local benchmark is used to make the measurement. If required, the local benchmark can be connected with a Ground Triangulation Survey (GTS) benchmark by carrying out levelling or by surveying with Total Station. Generally, the local benchmark is constructed by erecting a cement pillar very close to the study area. This can be referred to as a Permanent Bench Mark (PBM) when it is connected with GTS benchmark. If permanent structures like buildings, bridges, or jetties are available near the study area, they can be used as local benchmarks. In a place where a landslide occurs, it is better to establish two or three permanent benchmarks that cover the entire study area. The vertical height of the benchmark can be measured by levelling or using Total Station. With the availability of DGPS, the horizontal position of the benchmarks can be established; they are useful for locating the reference points in future.

A Total Station (manufactured by M/s Measurement Device Limited, UK) is an equipment that measures the distance and angle between two points by sending a laser beam from a point and letting it reflect from a target point. The time taken to traverse the distance permits accurate estimation of the distance. Simultaneously, horizontal and vertical angles are measured with respect to a reference point.

Autolevel (manufactured by M/s Nikon Corporation, Japan) is an equipment that is deployed to measure heights rapidly. Autolevel is first calibrated at known benchmarks and the survey is continued. The interval between two successive measurements depends on the nature of the terrain.

LaserTrak<sup>TM</sup> (manufactured by M/s Measurement Device Limited, UK) is another device that is used for measuring the distance between two points. The equipment can effectively be used for measuring a long distance from the station point.

The Automatic level or Dumpy level is used for precise levelling to determine the height of a location with reference to mean sea level or in the local reference framework. Position of a point can be determined using other suitable equipment or by conventional survey methods. Sometimes, height is

measured on the pre-marked grids, but this method is not suitable in a hilly terrain.

In case of hilly terrain, the Total Station or LaserTrak<sup>TM</sup> is useful to determine the topography. This is due to the steep slope or presence of trees in the vicinity. Total Station provides relative height and bearing with respect to a reference point and the distance, of a target point with respect to the station point. The geographical coordinate can be calculated based on the above data and co-ordinate of a base station. In case of Total Station fitted with a DGPS, the geographical coordinates can be obtained directly.

Land cover Category	Class	Weight for vegetation
0	Water	( <i>Null</i> )
1	Evergreen Needleleaf Forest	1
2	Evergreen Broadleaf Forest	1
3	Deciduous Needleleaf Forest	1
4	Deciduous Broadleaf Forest	1
5	Mixed Forest	1
6	Woodland	1
7	Wooded Grassland	3
8	Closed Shrubland	3
9	Open Shrubland	3
10	Grassland	3
11	Cropland	3
12	Bare Ground	6
13	Urban and Built	6

Table 1: Different land cover classifications used in GLCF land cover data (Hansen et al., 1998, 2000). Last column of the table show the different weights assigned to the vegetation re-classified map.



Soil unit	Type	Weight for bedrock-overburden contact	Weight for soil
1	Mixed, Typic Ustipsamment	1	4
2	Sandy, mixed, Typic Tropaquent	1	4
3	Fine loamy, mixed, Typic Tropaquent	1	4
4	Sandy, mixed, Typic Tropaquent	1	4
5	Fine,mixed, Aquic Ustropept	1	6
6	Fine,mixed, Fluventic Dystropept	1	6
7	Loamy-skeletal, mixed, Ustoxin Dystropep	1	3
8	Fine,mixed, Ustoxin Dystropept	1	3
9	Clayey-skeletal, mixed, Lithic Ustorthent	1	6
10	Clayey-skeletal, mixed, Lithic Ustorthent	1	3
11	Loamy-skeletal, mixed, Fluventic Ustropept	1	4
12	Fine-loamy, mixed, Typic Ustropept	1	4
13	Fine, mixed, Ustoxic Dystropept	1	4
14	Fine, mixed, Kanhaplic Haplustalf	1	4
15	Fine, mixed, Kanhaplic Haplustalf	1	4
16	Clayey-skeletal, mixed, Typic Ustropept	1	4
17	Fine loamy, mixed, Ustoxic Dystropept	1	4
18	Clayey-skeletal, mixed, Ustoxic Dystropept	6	6
19	Clayey, mixed, Lithic Dystropept	6	6
20	Clayey, mixed, Lithic Dystropept	3	4
21	Clayey-skeletal, mixed, Lithic Dystropept	6	6
22	Clayey, mixed, Typic Haplustult	3	3
23	Fine-loamy, mixed, Ustic Dystropept	6	6
24	Fine, mixed, Typic Ustropept	6	6
25	Fine, mixed, Typic Ustropept	6	6

Table 2: Soil classification as given in the soil map (Harindranath et al., 1999). Last two columns of the table show the different weights for bedrock-overburden contact and soil re-classified map. The weights assigned are derived from the soil map supplemented by the field observations in Kuskem.

<b>Factor/Parameter</b> ( <i>i</i> )	<b>Class</b> ( <i>i</i> )	<b>Ranks</b> ( $R_i$ )	<b>Weights</b> ( $W_i$ )
<b>Slope of the terrain</b>	0°–10°	6	1
	11°–20°		2
	21°–25°		3
	26°–30°		4
	31°–40°		5
	> 40°		6
<b>Height of the terrain</b>	0–50 m	5	1
	51–100 m		2
	101–150 m		3
	151–200 m		5
	> 200 m		6
<b>Vegetation (Land cover)</b>	Dense vegetation	4	1
	Sparse vegetation		3
	Barren		6
<b>Bedrock-overburden contact</b>	Transitional	3	1
	Semi-transitional		3
	Very sharp		6
<b>Soil type</b>	Hard laterite	2	0
	Laterite/Gravel		3
	Sands		4
	Clays		6
<b>Drainage pattern</b>	Low	1	1
	Medium		3
	High		6

Table 3: Ranks and weights of classes of parameters in Canacona taluka for computation of LPI.

<b>Factors</b>	$R_i$ and $W_i$ for maximum	$R_i$ and $W_i$ for minimum	$R_i * W_i$ (Maximum)	$R_i * W_i$ (Minimum)
<b>Slope of the terrain</b>	$R_i = 6$ $W_i = 6$	$R_i = 6$ $W_i = 1$	$6 * 6 = 36$	$6 * 1 = 6$
<b>Height of the terrain</b>	$R_i = 5$ $W_i = 6$	$R_i = 5$ $W_i = 1$	$5 * 6 = 30$	$5 * 1 = 5$
<b>Vegetation (Land cover)</b>	$R_i = 4$ $W_i = 6$	$R_i = 4$ $W_i = 1$	$4 * 6 = 24$	$4 * 1 = 4$
<b>Bedrock-overburden contact</b>	$R_i = 3$ $W_i = 6$	$R_i = 3$ $W_i = 1$	$3 * 6 = 18$	$3 * 1 = 3$
<b>Soil type</b>	$R_i = 2$ $W_i = 6$	$R_i = 2$ $W_i = 0$	$2 * 6 = 12$	$2 * 0 = 0$
<b>Drainage pattern</b>	$R_i = 1$ $W_i = 6$	$R_i = 1$ $W_i = 1$	$1 * 6 = 6$	$1 * 1 = 1$
<b>LPI value <math>\Sigma(R_i * W_i)</math></b>			<b>126</b>	<b>19</b>

Table 4: Example showing computation of maximum and minimum LPI values from the data presented in Table 3. It may be noted that the Landslide Potential Index (LPI) ranges from 19 to 126. Maximum and minimum LPI values indicate very high and very low landslide susceptible classes respectively.

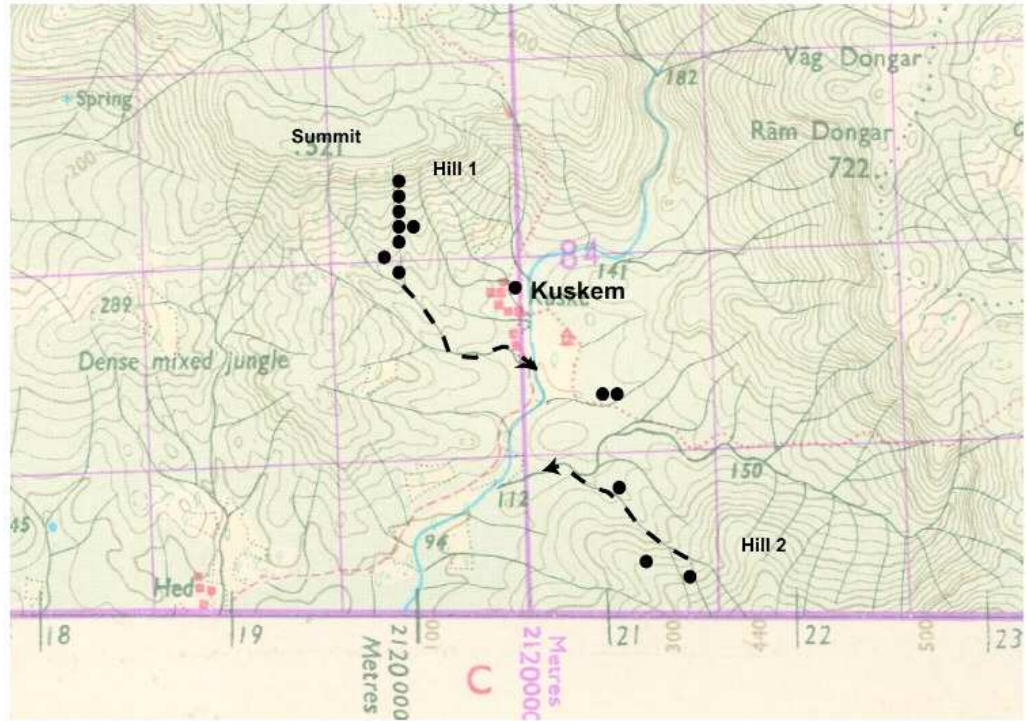


Figure 1: Map depicting the location of Hills 1 & 2. The solid dots depict the locations of observation and measurement. The dashed lines with arrow show approximate direction of the debris flow.



Figure 2: The photograph on the left shows NIO team in Kuskem village before climbing Hill 1. That on the right depicts the dried-up river channel along which the debris of landslide flowed down Hill 1. It depicts predominantly clayey composition of overburden and exposed bed rock at places.

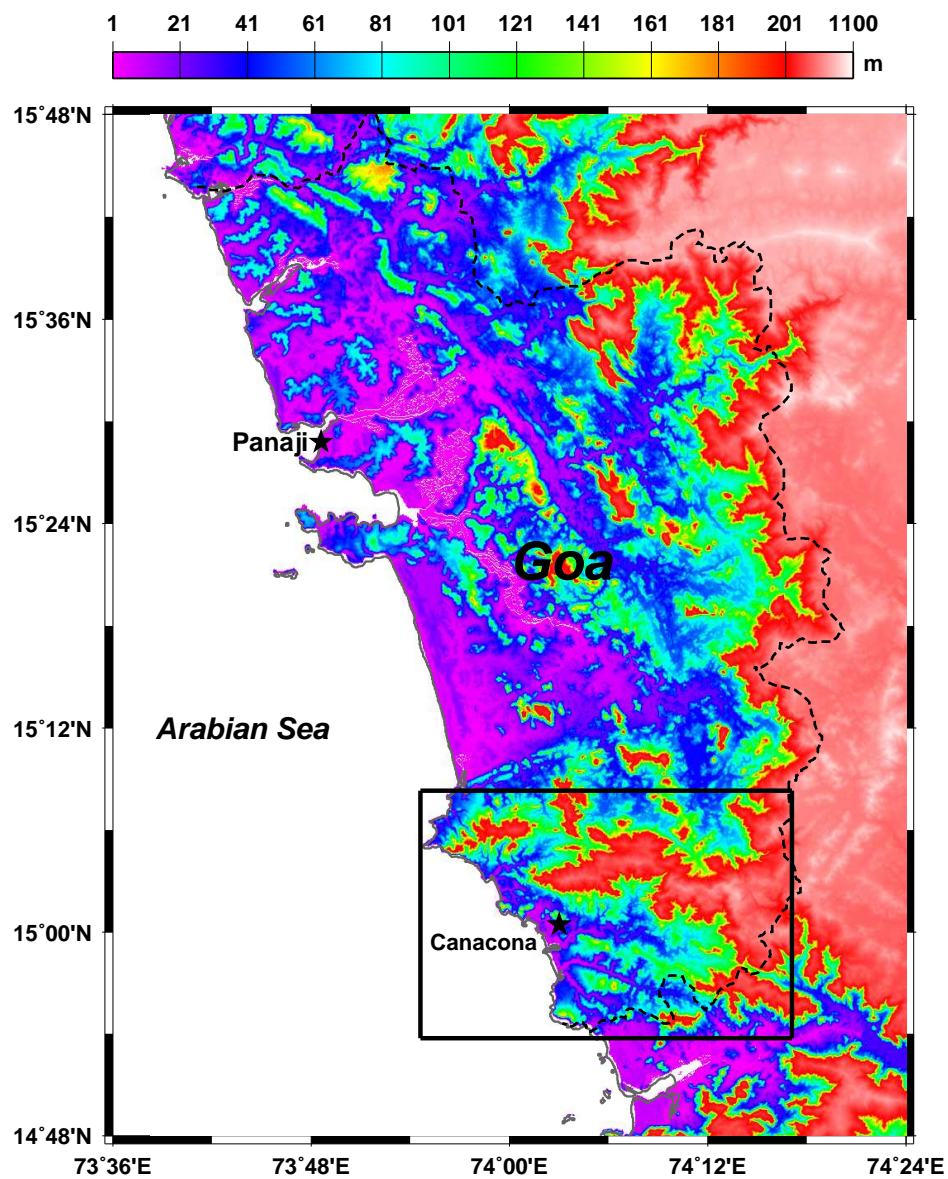


Figure 3: The topographic map of Goa from SRTM DEM. The colour scale at the top of the figure indicates elevation (m). The dashed black line marks the border of Goa. Canacona and its surrounding region is marked by the black rectangle. The landslide-susceptibility study has been carried out for this region.

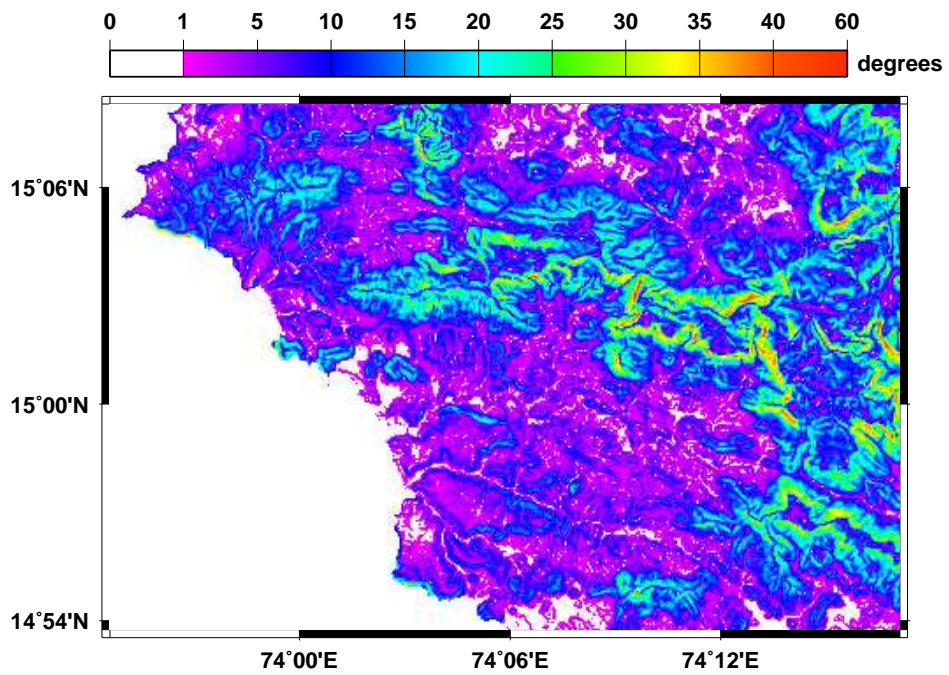


Figure 4: The slope map of Canacona region (region marked by the black rectangle in Figure 3) derived from the SRTM DEM. The colour scale at the top of the figure indicates slope (in degrees).

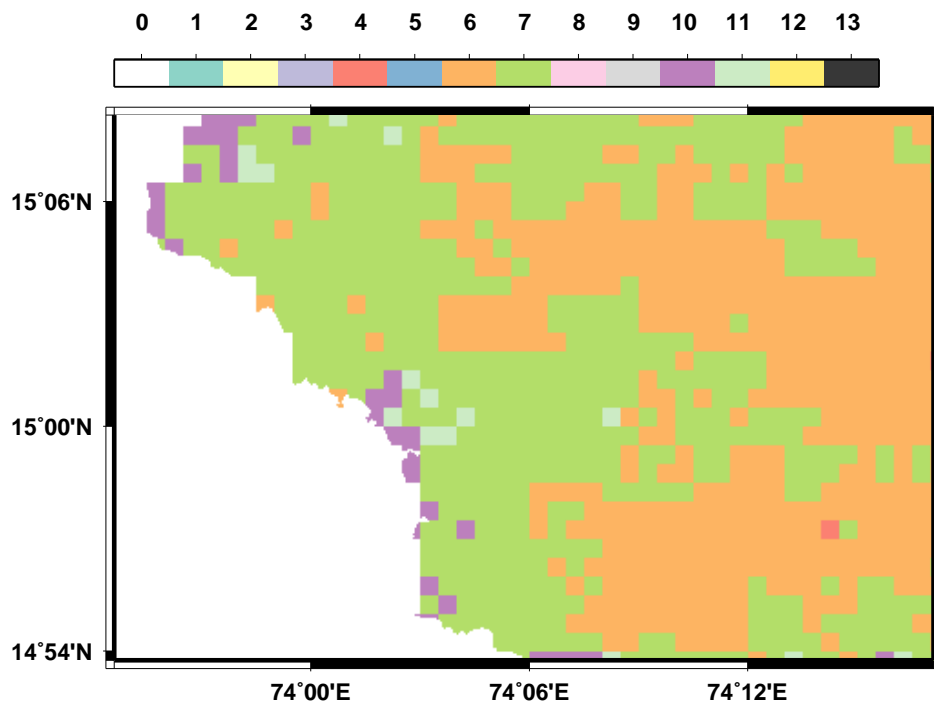


Figure 5: The land cover map of Canacona region (region marked by the black rectangle in Figure 3) derived from the Global Land Cover Facility's (GLCF) global land cover classification data. The colour scale at the top of the figure gives values for 14 different land cover categories (Table 1). The land cover map is re-sampled to conform to the SRTM grid as the original resolution of land cover data was 1 km.



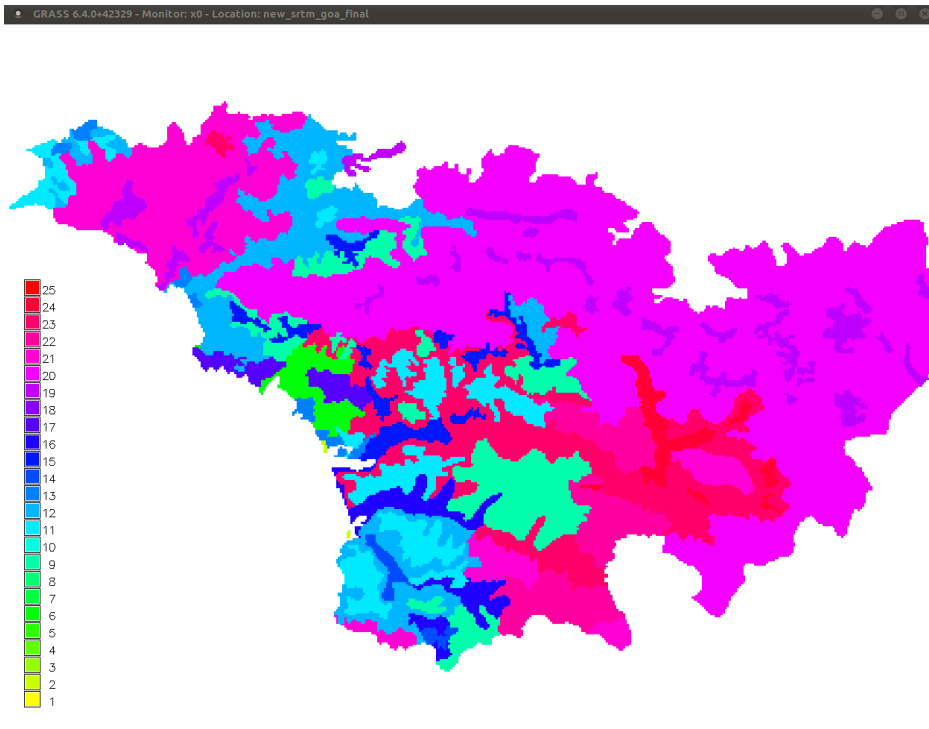


Figure 6: The digitised soil map of Canacona region (region marked by the black rectangle in Figure 3). The colour scale represents the soil type (Table 2). This map is used to derive both the soil and bedrock-overburden contact data.

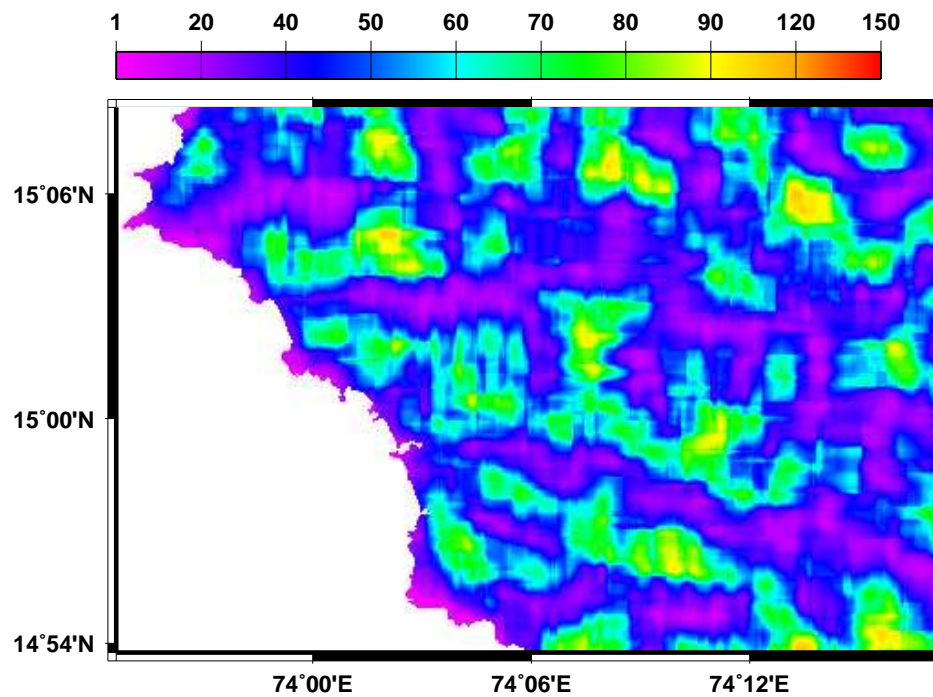


Figure 7: The drainage density map of Canacona region derived from the SRTM DEM. The colour scale at the top of the figure indicates the drainage density (number of stream grid cells in the neighbourhood of a given cell).

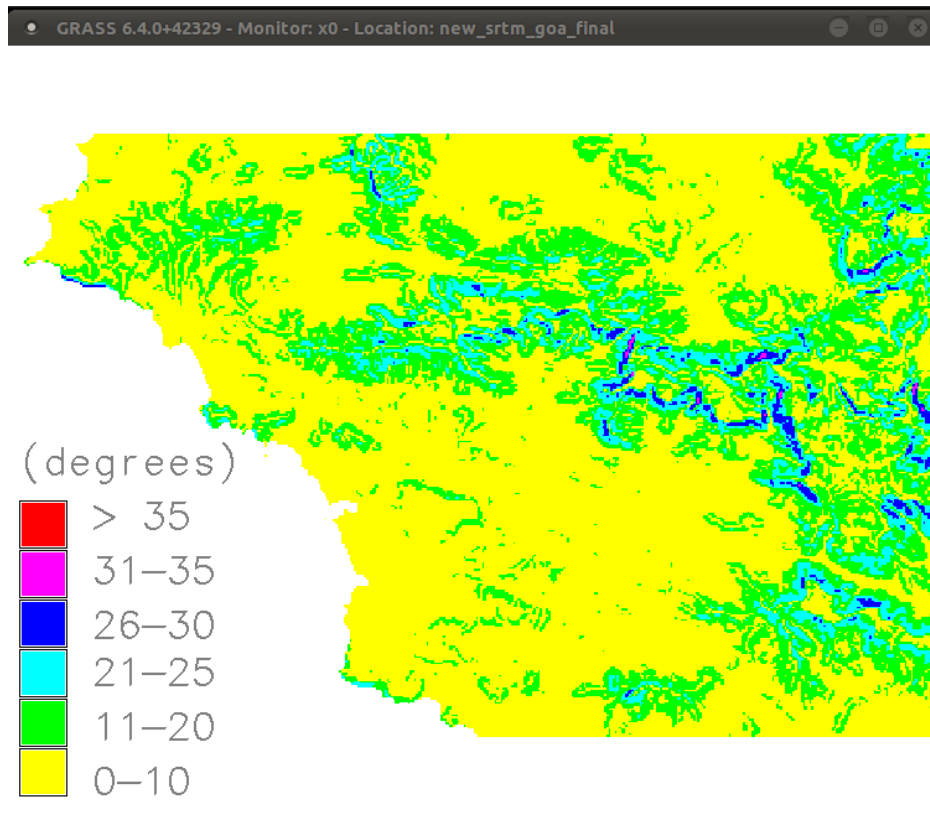


Figure 8: Re-classified slope map of Canacona region (region marked by the black rectangle in Figure 3). The colour scale represents the different classes based on slope angle.

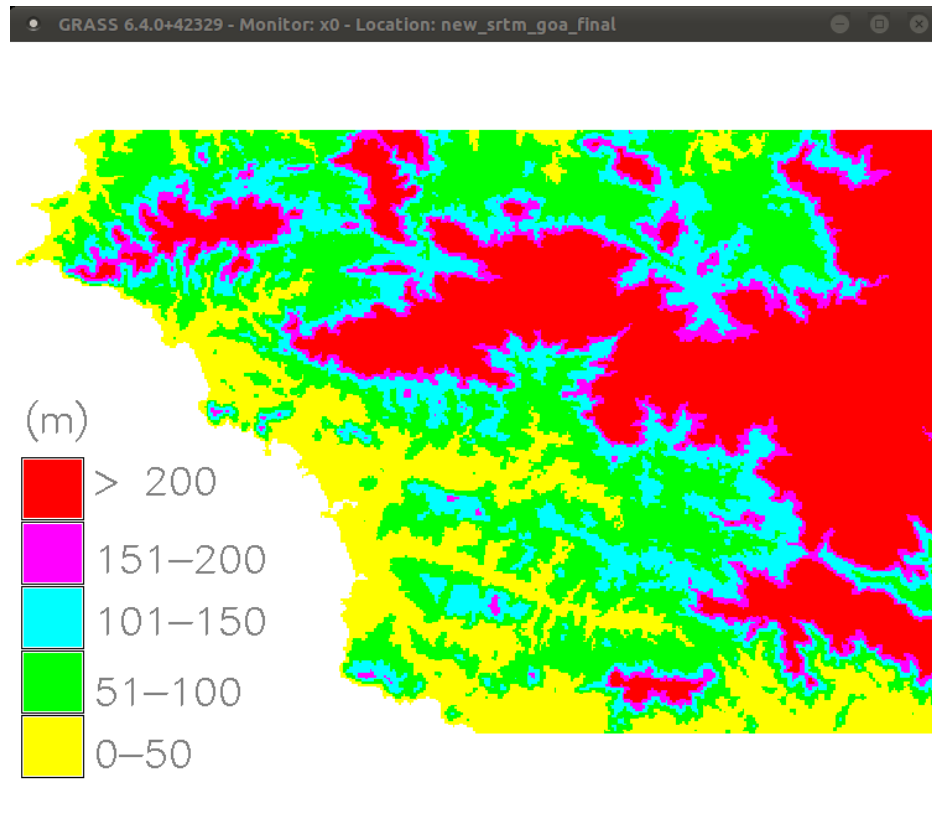


Figure 9: Re-classified topography of Canacona region (region marked by the black rectangle in Figure 3). The colour scale represents the different classes based on elevation (m).

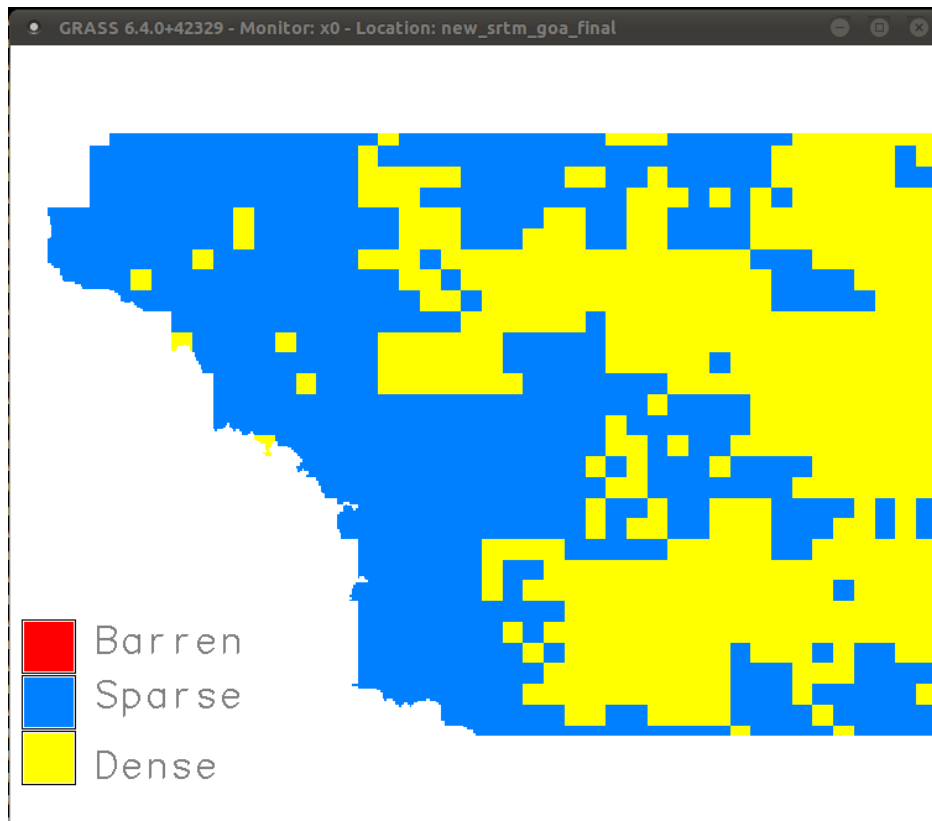


Figure 10: Re-classified land cover map of Canacona region (region marked by the black rectangle in Figure 3). The colour scale represents the different classes of vegetation. There is no barren land in this region.

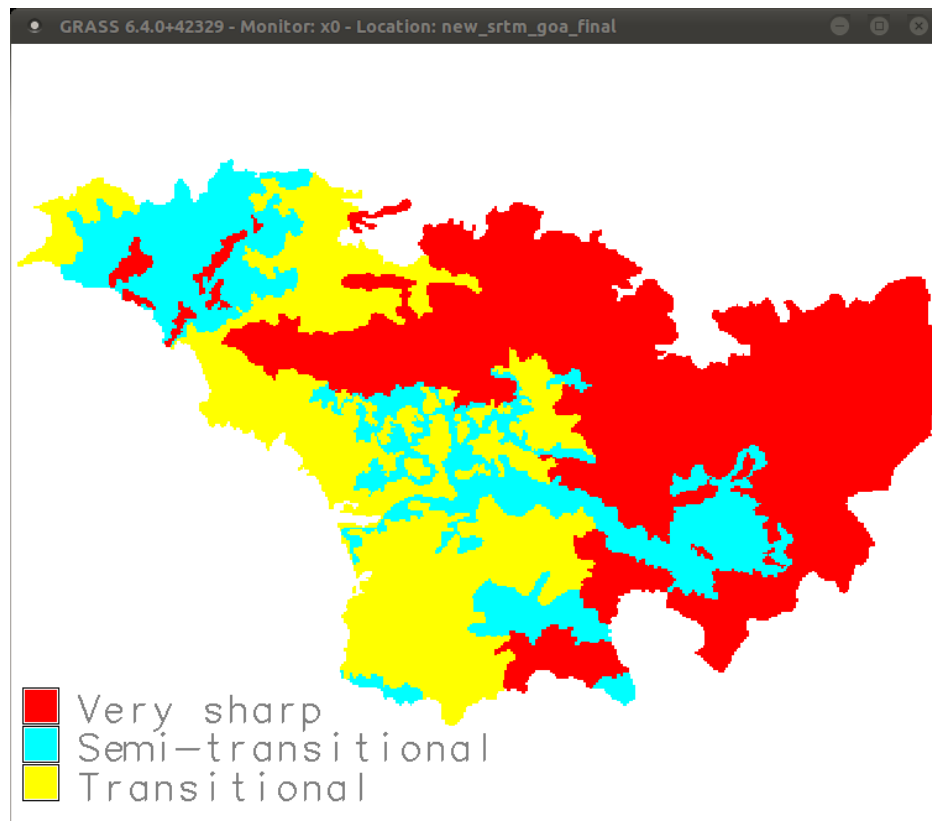


Figure 11: Re-classified bedrock-overburden contact map of Canacona region (region marked by the black rectangle in Figure 3) derived from the soil map. Information obtained from Kuskem field trip was crucial to identify bedrock-overburden contact classes from the soil map. The colour scale represents the different classes of bedrock-overburden contact.

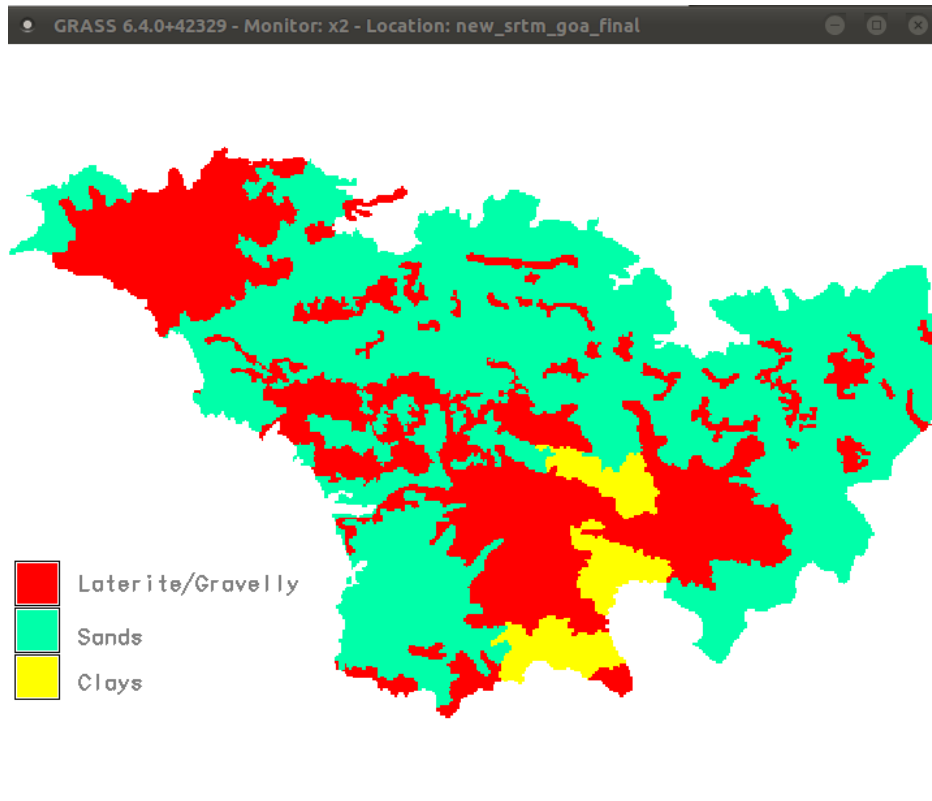


Figure 12: Re-classified soil map of Canacona region (region marked by the black rectangle in Figure 3). The colour scale represents the different soil classes (Harindranath et al., 1999).

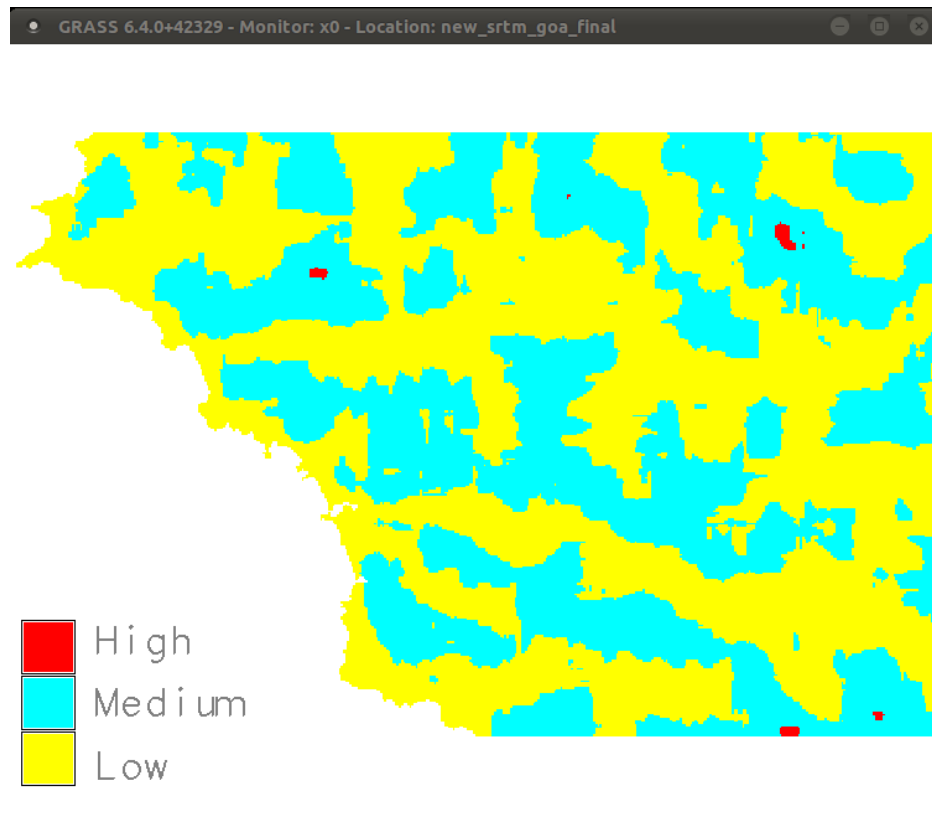


Figure 13: Re-classified drainage density map of Canacona region (region marked by the black rectangle in Figure 3). The colour scale represents the different classes of drainage density.



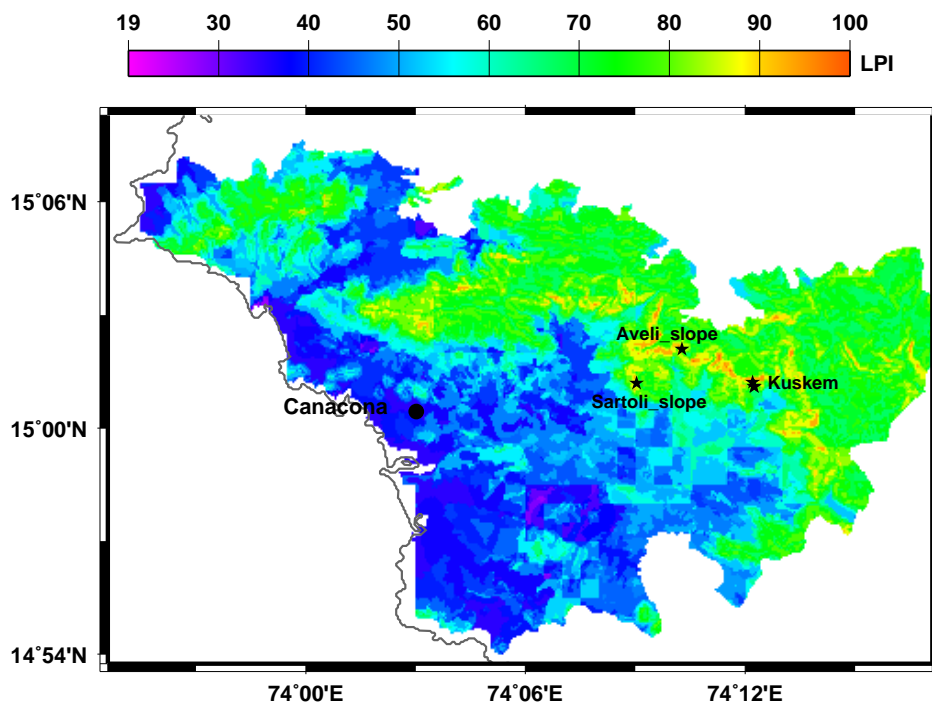


Figure 14: Landslide Potential Index (LPI) map derived for Canacona region (region marked by the black rectangle in Figure 3). The colour scale represents the LPI values (dimensionless). Locations where major landslides occurred on 2 October 2009 are marked on the map (black star). The locations coincide with high values of LPI (80–90).

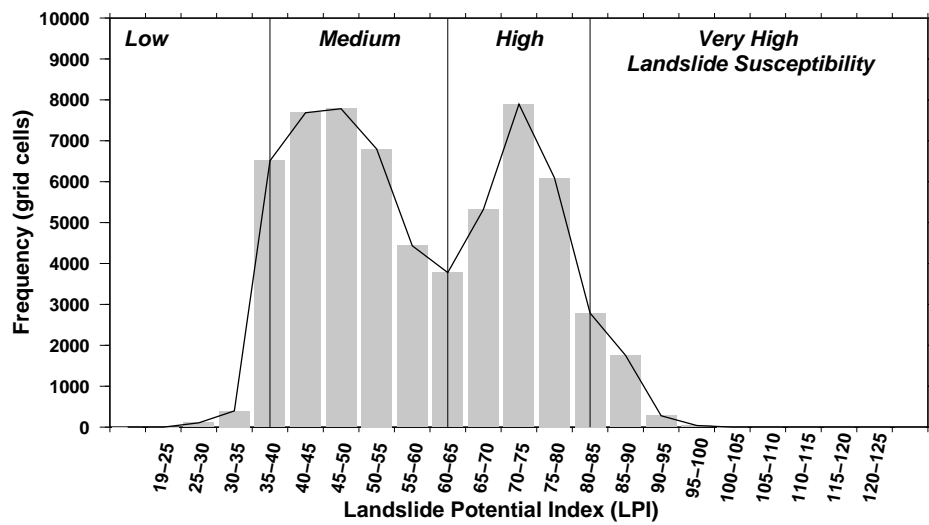


Figure 15: LPI-frequency graph showing the LPI values in the Canacona region (region marked by the black rectangle in Figure 3). The LPI-frequency graph shows the number of grid cells (frequency, ordinate) that had a LPI value in the bands marked on the abscissa. Vertical lines drawn on the graph represent LPI thresholds for very high, high, medium and low landslide-susceptibility.